

INVESTIGATION OF THE RADIOACTIVITY  
OF TERBIUM 160

by

VAHE KESHISHIAN

B.S., Kansas State College  
of Agriculture and Applied Science, 1952

---

A THESIS

submitted in partial fulfillment of the

requirements for the degree

MASTER OF SCIENCE

Department of Physics

KANSAS STATE COLLEGE  
OF AGRICULTURE AND APPLIED SCIENCE

1954

LD  
2668  
T4  
1954  
K45

107

C.2  
Documents

TO  
MY MOTHER

## TABLE OF CONTENTS

INTRODUCTION.....	1
EXPERIMENTAL APPARATUS .....	7
The Magnets .....	7
Beta-Ray Spectrographs.....	10
The Variable Radius Beta-Ray Spectrometer .....	10
Radioactive Source Assemblies.....	13
PHOTOELECTRIC RADIATORS.....	14
EXPERIMENTAL RESULTS.....	26
ACKNOWLEDGMENTS.....	36
LITERATURE CITED.....	37

## LIST OF ILLUSTRATIONS AND TABLES

Plate I	Photograph of High Field Magnet and Large Beta-Ray Spectrograph...	6
Plate II	Photograph of Low Field Magnet and the Variable Radius Beta-Ray Spectrometer.....	9
Plate III	Photograph of Small Beta-Ray Spectrograph and Source Assembly in Position.....	12
Plate IV	Spectrograms Obtained with Ir <sup>192</sup> and Various Radiators.....	17
Plate V	Front View and Back View of Radiator Holder.....	19
Plate VI	Spectrograms Obtained with Ir <sup>192</sup> source and Lead Radiators of Different Thicknesses.....	23
Plate VII	Spectrogram of Tb <sup>160</sup> in High Energy Region.....	25
Plate VIII	Fermi-Kurie Plot of Tb <sup>160</sup> .....	28
Plate IX	Normalized Beta Spectrum of Tb <sup>160</sup> .....	30
Plate X	Proposed Decay Scheme of Dy <sup>160</sup> .....	33
Table 1	Observed Gamma-Rays of Dy <sup>160</sup> .....	35

## INTRODUCTION

One of the most important problems in nuclear physics today is to find a hypothesis for the structure of the nucleus of an atom. Many theories have been proposed, but as none of them give a complete picture of the nucleus, much research is being done at the present time along this line.

Most of the present knowledge about the nucleus is derived from data obtained from scattering experiments, mass spectroscopy, beta-ray and gamma-ray spectroscopy. Although extensive research has been done with odd-even and odd-odd nuclei in the field of beta-ray spectroscopy, the beta-ray spectroscopy of even-even nuclei is in a much less developed state. The present research has consequently been directed towards nuclei of this last type. The particular radio-isotope which is the subject of this report is  $Tb^{160}$ . This isotope decays by beta-minus emission to the even-even nucleus  $Dy^{160}$ .

The ultimate objective of this investigation has been to propose a decay scheme of  $Dy^{160}$  with the appropriate spin and parity assignments. The major method of investigation has been that of beta-ray spectroscopy.

The application of beta-ray spectroscopy to the problem of energy level diagram construction comes about in the following manner. As is well known, nuclei are capable of existing in only discrete energy levels. In the present instance, the  $Dy^{160}$  which followed beta-minus emission of  $Tb^{160}$ , is actually in a highly excited state. Almost immediately after formation, however, it decays to its ground state, passing in transit through a series of discrete energy levels. The energy released, when the nucleus falls from one level to a lower one, is emitted as gamma radiation, or as kinetic energy of a monoenergetic orbital electron. These electrons are called internal conversion

electrons. The energy of the gamma-ray is just the energy difference of the two levels. For the conversion electrons, the energy is likewise that of the energy difference of the two levels minus the binding energy characteristic of the particular orbit from which the electron was removed.

The construction of energy level diagrams from the beta-ray or gamma-ray spectroscopy standpoint, is essentially a problem of synthesis. The observed gamma-ray energies are really differences of energy between levels. The energy differences are then synthesized into an energy level diagram.

Gamma-ray energies may also be measured by application of the photoelectric effect. In this method the gamma-rays are allowed to impinge upon a radiator in which they may give up their entire energy to tightly bound orbital electrons belonging to the atoms of the radiator. A measurement of the energy of the ejected electron thus gives that of the gamma-ray when the binding energy characteristic of the orbit is added to the electron energy. For reasons to be discussed later, it is frequently advantageous to employ several different radiators. In the present investigation, for example, radiators of U, Pb, Pt, Ta, Sn, and Mo were employed.

It was mentioned earlier that  $\text{Dy}^{160}$  was formed after beta-minus emission from  $\text{Tb}^{160}$ . As is well known, beta particles (or electrons) emitted by such nuclei are not monoenergetic, but instead have energies distributed over a spectrum ranging from zero to a maximum energy. The maximum energy is also a transition energy linking the two nuclides, and is therefore of interest.

In the present investigation, energies of conversion electrons and photoelectrons were obtained by using three different  $180^\circ$  beta-ray spectrographs. The continuous beta spectrum was studied with a variable radius beta-ray spectrometer. These instruments will be discussed in detail in the

following section.

The operating principle for a 180° beta-ray spectrograph or a variable radius beta-ray spectrometer hinges upon the fact that an electron with a velocity  $\underline{v}$  perpendicular to a magnetic field  $\underline{B}$ , is acted upon by a force  $\underline{F}$  that results in a circular motion of the electron in a plane perpendicular to the field. The following equations are applicable to this situation.

$$\underline{F} = e \underline{v} \times \underline{B} \quad (1)$$

The terms in this equation are given as follows:

$F$ -the normal force acting on the electron in dynes.

$e$ -the charge of the electron in e.m.u.

$v$ -the velocity of the electron in cm/sec.

$B$ -the magnetic field intensity in gaussses.

The trajectory resulting from the force is circular with a radius of curvature  $\rho$  is given by,

$$\rho = \frac{mv}{Be} = \frac{m_0 v}{Be \left[ 1 - \left(\frac{v}{c}\right)^2 \right]^{\frac{1}{2}}} \quad (2)$$

The symbols here have the following meanings:

$\rho$ -the radius of curvature of the electron path in cm.

$m$ -the dynamic mass of the electron in grams.

$m_0$ -the rest mass of the electron in grams.

$c$ -the velocity of light in cm/sec.

The kinetic energy  $E$ , in ergs is given by,

$$E = mc^2 - m_0c^2 = m_0c^2 \left\{ \left[ 1 - \left(\frac{v}{c}\right)^2 \right]^{-\frac{1}{2}} - 1 \right\} \quad (3)$$

An explicit solution combining equations (2) and (3) gives,

$$E = \left[ (m_0c^2)^2 + B^2 \rho^2 e^2 c^2 \right]^{\frac{1}{2}} - m_0c^2 \quad (4)$$

To three place accuracy, equation (4) may be written, using the best available values of the physical constants  $m_0c$ , and  $e$ ,

$$E' = \left\{ .511^2 + \left[ \frac{2E\rho}{104} \right]^2 \right\}^{\frac{1}{2}} - .511 \quad (4)'$$

Here  $E'$  is in Mev.

In the form of equation (4)', the energy  $E'$  is displayed as a function of the product of the magnetic field intensity  $B$ , and the radius of curvature of the electron path.

In applications of the  $180^\circ$  type beta-ray spectrographs, a uniform field  $B$  is adjusted to a value suitable to the focusing range of the spectrum and held constant so that energies of the electrons become functions of  $\rho$  only.

The energy determination of monoenergetic electron groups is particularly simple, since the electrons focus with essentially a single value of  $\rho^1$ . Accurate measurements of these radii are simple and with a knowledge of the magnetic field, they lead directly to the electron energies. The energy values of the parent gamma-rays associated with the electron groups are then obtained by adding the appropriate binding energies to the electron energies.

---

<sup>1</sup>Actually, some of the electrons leaving the radioactive sources do not emerge perpendicular to the magnetic field. This, as well as some other factors, prevent the electrons from all focusing at one value of  $\rho$ . In the  $180^\circ$  beta-ray spectrographs, the focussed image of the source appears roughly as a line on a photographic plate. For this reason, "conversion line" has become synonymous with conversion group in beta-ray spectroscopy.



EXPLANATION OF PLATE I

Fig. 1. Photograph of the high field magnet with large spectrograph.

Fig. 2. A close-up view of the large spectrograph.

## PLATE I



Fig. 1



Fig. 2

## EXPERIMENTAL APPARATUS

In this section are given descriptions of the various instruments and accessories that were employed in this research. In some cases, easily available references are cited in place of detailed discussions. The components so described include the constant field magnets, the beta-ray spectrographs, the variable radius beta-ray spectrometer, and the radioactive source assembly.

## The Magnets

The two constant field magnets, employed for the spectrographs and spectrometer, as seen in Plate I, Fig. 1, and Plate II, Fig. 1, are essentially those described by Kruse (7). One of the magnets described by Kruse was altered so that the maximum field attained was increased from 600 gauss to 800 gauss. This was done by lowering the top pole face, which reduced the air gap from 7.8 cm. to 4.6 cm. In both magnets once the fields were established and stabilized, no appreciable changes in field values were observed over a period of many months.

The magnetic fields were calibrated with the use of K-conversion lines arising from the following accurately determined gamma-ray energies: 67.7, 100.1, 264.1, 1122.0 and 1222.1 Kev of  $W^{182}$ , 316.5 and 604.5 Kev of  $Pt^{192}$ . These values were obtained by Muller et al (8). The 876 Kev gamma-ray of  $Tb^{160}$  as reported by Cork et al (4) was also employed as a calibration standard occasionally. These standard values were so spaced as to allow good calibration over a wide range of energies.

For regions up to 12 inches in diameter in the central portion of the pole gap the fields of both magnets were quite uniform. The uniformity was

EXPLANATION OF PLATE II

Fig. 1. Photograph of the low field magnet, variable radius spectrometer and scalar.

Fig. 2. Interior view of the variable radius spectrometer.

## PLATE II



Fig. 1



Fig. 2

ascertained by comparison of different energy standards with the same field.

### Beta-Ray Spectrographs

Of the three  $180^\circ$  beta-ray spectrographs used, two of them, as seen on Plate III, Fig. 1, are essentially those described by Kruse (7). The source assembly holders were modified in such a way that the source assemblies of various isotopes could be interchanged readily and quickly in a short time. Plate III, Fig. 2, shows the position of the source assembly holder. It can be observed that the source assembly was attached to the holder by only one screw on the right side.

A third spectrograph was constructed for use in the high field magnet, as shown on Plate I, Fig. 2. The external dimensions were 38.5 cm. by 30.5 cm. and 4.6 cm. high. The base and the lid were  $1/4$  inch thick, whereas the walls were  $3/8$  inch thick. All these components were cut from brass plates. The method of source mounting was identical to that of the two previously described spectrographs.

The maximum energy which could be measured with the spectrographs were as follows. The two small spectrographs, when placed in a magnetic field of 550 gauss, could measure energies up to 1.7 Mev. The large spectrograph, when placed in a magnetic field of 800 gauss, could measure energies up to 3.3 Mev.

### The Variable Radius Beta-Ray Spectrometer

The variable radius spectrometer, with a few modifications discussed below, has been described by Kruse (7). A view of the interior is shown on Plate II, Fig. 2. Only one geiger tube was employed, whereas two were used in the spectrometer described by Kruse. The source mounting was also changed

EXPLANATION OF PLATE III

Fig. 1. Photograph of small spectrograph with source in position.

Fig. 2. Close-up rear view of source assembly in position.

## PLATE III



Fig. 1



Fig. 2



in the same manner as described in the previous section. The lead block shown in this figure shielded the geiger tube from the source gamma radiation.

The geiger tube filling gas consisted of a mixture of alcohol vapor and argon, to a total pressure of approximately 12 cm. An alcohol supply kept at 0° C. was continually opened to the gas system. This fixed the partial pressure of the alcohol at its 0° C. vapor pressure of 1.2 cm.

#### Radioactive Source Assemblies

Sources for analysis of internal conversion electrons and the continuous beta spectrum were prepared in the following manner. The radioactive  $Tb^{160}$  in the form of a powdered oxide, was applied to the adhesive side of a narrow strip of scotch tape, about 1 mm. wide. This strip was then taped to the middle of an aluminum frame. This source assembly was then secured to the source assembly holder by a small screw. The mounted source assembly may be seen on Plate III, Fig. 2. As also seen in Fig. 2, the source assembly is mounted in such a fashion that the source strip is perpendicular to the spectrograph base, and thus parallel to the magnetic field. One advantage of this type of source mounting was that a source assembly could be used interchangeably in all the spectrographs and in the spectrometer.

For photoelectric studies, much stronger sources are usually required to keep exposure times within reasonable limits, since the cross-sections for photo-electron production are quite small. In the present investigation, sources for photoelectric studies were prepared in the following manner. A large quantity (several milligrams of  $Tb^{160}$ ) was applied to the middle of a 1 cm. wide scotch tape strip then another strip of scotch tape was placed on top of it such that the source was sandwiched between the two strips of scotch

tape. The source width was about 3 mm. while the length was about 2 cm. The source density of approximately  $10 \text{ mg/cm}^2$  was considerably greater than those of internal conversion sources.

#### PHOTOELECTRIC RADIATORS

Photoelectron analysis of gamma-rays was useful for several reasons. As described later, such analysis served to distinguish between K and L conversion lines, to determine gamma-ray energies less than 100 Kev, and finally as a means of identifying gamma rays whose conversion lines were obscured.

Preliminary to the application of photoelectron analysis of  $\text{Tb}^{160}$ , an investigation was undertaken to determine which radiators were the most effective in given energy ranges, and also to determine optimum radiator thicknesses.

A very strong  $\text{Ir}^{192}$  source was used in this preliminary investigation. This strong source allowed a great reduction in exposure time over that required for most other available sources.

Before proceeding with a discussion of the results obtained, a brief review is given of some of the principles involved in the photoelectric effect. Gamma-rays give up their energies to bound K, L, M shell electrons of the radiator. These electrons, in turn, leave the atom with the kinetic energy of the parent gamma-ray, minus the binding energy of the particular orbital electron. As the photoelectric absorption cross-section for K shell electrons is much greater than that for the L and M shell electrons, only the photoelectric absorption coefficient for K shell electrons was considered in the calculations involved in these experiments.

Use was made of an approximate equation which showed that the photoelectric coefficient of absorption was proportional to the fifth power of the atomic number of the radiator (5). The absorption coefficient also varied with the gamma-ray energy, but as the investigation undertaken here involved the same group of gamma-ray energies for the different radiators, this factor could be omitted from consideration.

Plate IV shows a series of spectrograms obtained with the  $\text{Ir}^{192}$  source employing four different radiators, U, Pb, Pt, and Ta. The four spectrograms are so positioned, that equal horizontal distances along the films from the left edge correspond to the same energy, i. e. energy increases towards the right. Although other lines are visible on the plates, only those marked K and L which arise from K and L orbital electrons ejected by a gamma-ray of 316.4 Kev, are considered in the following discussion. It can be seen that the L lines are not displaced much. This is to be expected since the L binding energies for the four radiators vary only from 17.1 to 9.8 Kev. Thus the energy range of the photoelectrons is from 299.3 to 306.6 Kev. On the other hand, the K lines show a considerable shift since the K binding energies vary from 115.0 Kev for U to 67.4 Kev for Ta, and thus the photoelectron energies range from 201.4 to 249.0 Kev. The comparatively large shift of a K line as compared to that of an L line was useful when some doubt existed as to whether a conversion line arose from a K or L shell. This technique was also of help when a K line of a given gamma-ray was obscured by the presence of an L line from another gamma-ray.

A special radiator holder was designed and constructed with adjustable lucite slits, which served to define the radiator width. The slits could be set at widths from .5 mm to 1.5 mm. By proper choice of the radiator width,

EXPLANATION OF PLATE IV

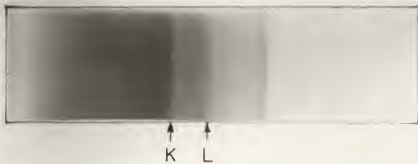
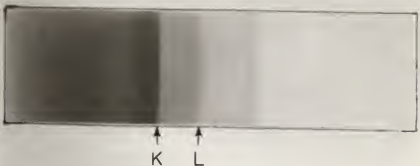
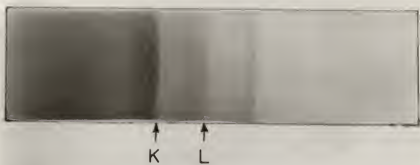
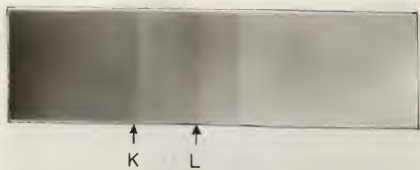
Fig. 1. Spectrogram of Ir<sup>192</sup> with uranium radiator. Exposure time:  
30 min.

Fig. 2. Spectrogram of Ir<sup>192</sup> with lead radiator. Exposure time:  
66 min.

Fig. 3. Spectrogram of Ir<sup>192</sup> with platinum radiator. Exposure time:  
80 min.

Fig. 4. Spectrogram of Ir<sup>192</sup> with tantalum radiator. Exposure time:  
133 min.

## PLATE IV



EXPLANATION OF PLATE V

Fig. 1. Front view of radiator holder.

Fig. 2. Back view of radiator holder mounted on lead block, with lead radiator and source.

## PLATE V



Fig. 1

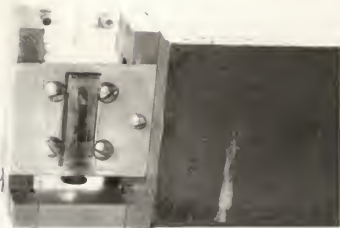


Fig. 2

optimum photographic resolution could be obtained. Plate V shows two views of the radiator holder. The vertical scotch tape source can also be seen. The dark sheet located immediately behind the slits is the radiator. As normally employed, the source was butted against the radiator, and behind the radiator and slit opening.

The radiator holder was a valuable adjunct to this investigation because of the simplicity with which radiators and sources could be changed, while still retaining precise radiator dimensions.

Referring back to Plate IV, it should be noted that the relative intensities of the photoelectric lines are approximately equal. This rough equality of intensity was brought about by adjusting the exposure time for the different plates. As would be expected from the large atomic number, the U radiator exposure was least, while Ta, with the smallest atomic number required the greatest exposure. Thus, from the standpoint of exposure time, U should serve as the most effective radiator. However, elements with atomic numbers greater than that of lead are naturally radioactive. Although such radiators are frequently employed, it was decided not to use them in the actual research with  $Tb^{160}$ , since a uranium radiator, for instance, would act as a weak source in itself. It was thus concluded that lead was the best radiator for energies greater than 100 Kev. Below 100 Kev, lead as a radiator becomes increasingly less useful, since its K binding energy is around 88 Kev, and the energies of the K photoelectrons become too small for effective photographic plate sensitization.

Some investigations of radiators with atomic numbers less than that of tantalum were made. For energies greater than 200 Kev, the Compton background became so intense that photoelectron lines were difficult to observe.



This is in agreement with the theory which predicts that the ratio of the coefficient of photoelectric absorption to that of Compton absorption decreases with decreasing atomic numbers, and also decreases with increasing energies.

For gamma-ray energies from about 30 to 100 Kev, tin and molybdenum were found to be the best suited as their K binding energies are 29.1 and 20.0 Kev respectively. In the investigation of  $Tb^{160}$ , tin and molybdenum were used exclusively to determine energies below 65 Kev. Since Dy has a K binding energy of 53.7 Kev, and photographic plate sensitivity requires at least 12 Kev for electrons, it is seen that 65 Kev gamma-rays are near the minimum for production of detectable K conversion electrons. Although L conversion lines can be observed for gamma-rays below 65 Kev, difficulties arise in differentiating  $L_1$ ,  $L_2$ , and  $L_3$  subshell lines. The presence of Auger electrons presents another complicating factor in this energy region.

Plate VI shows a series of spectrograms, all taken with lead radiators, but with varying radiator thicknesses. Radiator thicknesses ranged from .0017 cm (the top spectrogram) to .0262 cm (the lower spectrogram). The same exposure times were used for all spectrograms. The intensities of the lines are roughly the same for all plates. This can be explained in the following way. Most of the photoelectrons produced in the inner lead layers are absorbed by a layer in front of them, since lead is a very good absorber of electrons. Consequently, in all of the spectrograms shown on Plate VI, only the outer lead layers of the radiator were effective in photoelectron line formation. Thus, it was concluded that for lead, the thickness of the radiator was immaterial, at least for lower energies.

EXPLANATION OF PLATE VI

- Fig. 1. Spectrogram of  $\text{Ir}^{192}$  with lead radiator. Lead thickness: 0.0017  
cm. Exposure time: 2 hours.
- Fig. 2. Spectrogram of  $\text{Ir}^{192}$  with lead radiator. Lead thickness: 0.0030  
cm. Exposure time: 2 hours.
- Fig. 3. Spectrogram of  $\text{Ir}^{192}$  with lead radiator. Lead thickness: 0.0064  
cm. Exposure time: 2 hours.
- Fig. 4. Spectrogram of  $\text{Ir}^{192}$  with lead radiator. Lead thickness: 0.0114  
cm. Exposure time: 2 hours.
- Fig. 5. Spectrogram of  $\text{Ir}^{192}$  with lead radiator. Lead thickness: 0.0262  
cm. Exposure time: 2 hours.

## PLATE VI



Fig. 1



Fig. 2



Fig. 3



Fig. 4



Fig. 5

EXPLANATION OF PLATE VII

Spectrogram of  $\text{Tb}^{160}$  in high energy region. The two strong conversion lines on the extreme right arise from 1173 and 1266 Kev gamma-rays.

PLATE VII



## EXPERIMENTAL RESULTS

$Tb^{160}$  decays by beta emission to an excited state of  $Dy^{160}$ , and then through a series of gamma-rays to its ground state. Most of the gamma-ray energies listed by Cork et al (3,4) and by Burson et al (2) were observed. Many additional gamma-rays were observed in this investigation. In particular, two intense gamma-rays were found beyond the strong 962 Kev gamma-ray, not recorded by these other observers. Energies of these two gamma-rays are 1173 Kev and 1266 Kev. Plate VII shows clearly these two strong lines together with the previously known strong 876 Kev and 962 Kev conversion lines.

Plate VIII shows the Fermi-Kurie plot of  $Tb^{160}$ . This plate clearly indicates several individual spectra, whose endpoint energies were found to be  $851 \pm 5$ ,  $557 \pm 10$ ,  $460 \pm 15$ , and  $280 \pm 20$  Kev. The last one of these has been designated as questionable due to the interference of the L and M conversion lines of the strong 297 Kev gamma-ray with the total beta spectrum. Data for the Fermi analysis of these spectra were obtained with the variable radius spectrometer. Details of the procedure employed are given by Klots et al (6).

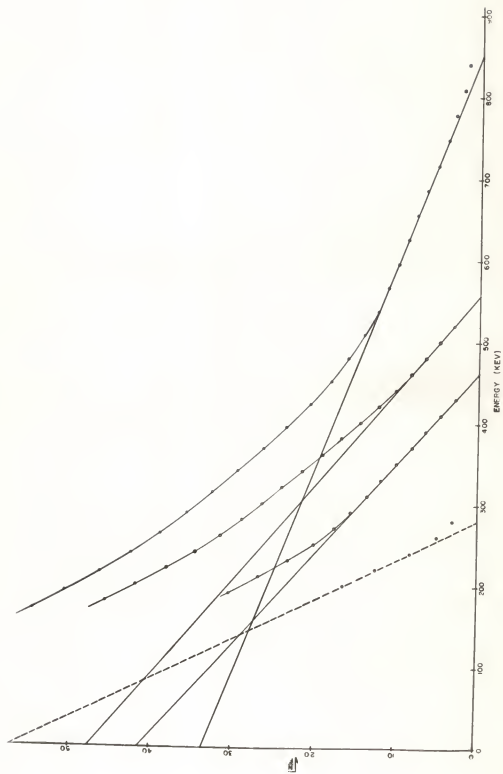
The relative intensities of the above mentioned spectra were obtained in the usual manner, by renormalizing the spectral data of Plate VIII. The relative abundances calculated from the spectra were 30, 32, 19, and 19 per cent for the 851, 557, 461 and 280 Kev groups of beta-rays respectively. The four beta transitions decaying at independent rates combine to give the experimentally observed half-life of  $72.2 \pm .5$  days.

Plate IX shows the normalized composite spectrum, made up of the four separate components. Also shown on this plate is a portion of the high energy conversion electron spectrum. The two largest peaks are the K conversion

EXPLANATION OF PLATE VIII

Fermi-Kurie plot of  $Tb^{160}$ , showing presence of four beta spectra.

PLATE VIII

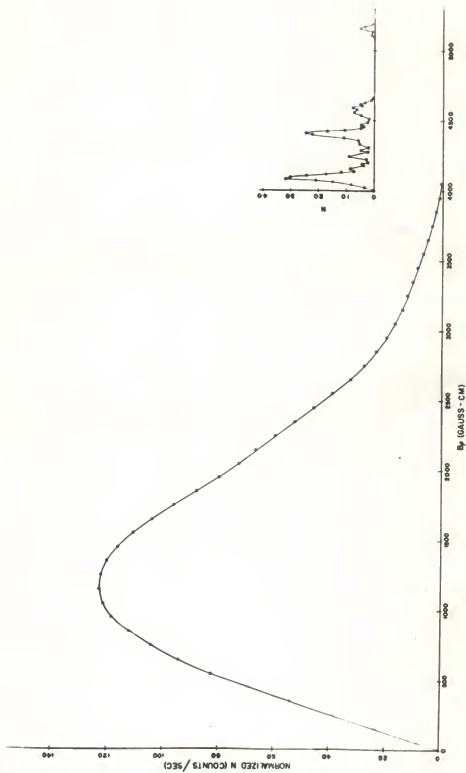




EXPLANATION OF PLATE IX

Normalized composite beta-spectrum of  $Tb^{160}$ .

PLATE IX



lines for the 876 and 962 Kev gamma-rays. The peak at the far right is the K conversion line for the 1173 Kev gamma-ray.

Incidentally, the lack of appearance of any different half-life components over a period of nine cycles is good evidence that no contaminants were present in the radioactive sources investigated.

The proposed decay scheme, Plate X, differs from those proposed by Cork et al (4) and Burson et al (2). There is some similarity, however, between the proposed scheme and that given by Cork. Four new levels have been added. Two levels of the Cork scheme at 375 and 673 Kev have been deleted. Levels G and H, on Plate X, are felt to be fairly certain, since their values were determined by the intense 1173 and 1266 Kev gamma-rays. Levels F and J are somewhat less certain since the gamma-rays leading to these positions are markedly weaker. However, it is noted that level J received some support from the beta spectrum analysis.

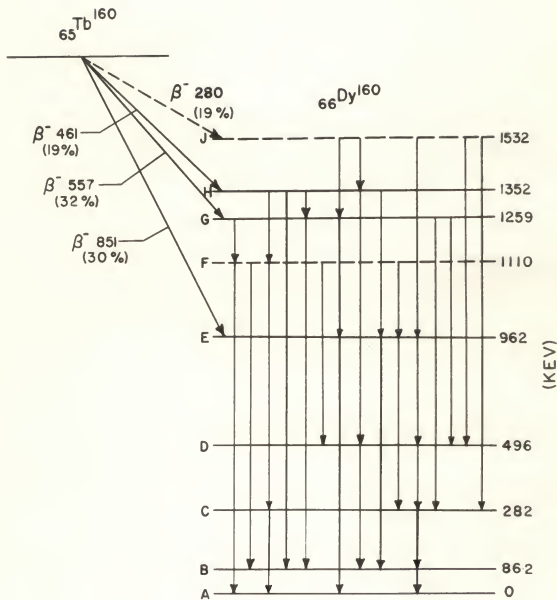
It was not possible to determine multipole orders for the radiations since the conversion coefficient ratios  $\alpha_K/\alpha_L$  obtained experimentally were subject to errors of at least 15 percent. In the energy regions considered here, precision of the order of 1 to 2 percent would have been necessary to distinguish multipolarity from the  $\alpha_K/\alpha_L$  ratios.

Spin and parity assignments were given to only four levels. The values so assigned were,  $0^+$  for level A,  $2^+$  for level B,  $4^+$  for level C, and  $1^-$  for level E. It is suspected that level D might have an assignment of  $6^+$ . These assignments were not based upon direct experimental evidence observed here. If the lower three levels A, B and C have the values assigned, then this portion of the decay scheme fits very well the Bohr-Mottelson (1) predictions for low lying levels in spin, parity and energy. Level D, according to

EXPLANATION OF PLATE I

Proposed decay scheme of Dy<sup>160</sup>.

## PLATE X



the Bohr-Mottelson theory should be somewhat higher in energy, and should be classified  $6+$ . The spin-parity assignment of  $1-$  for level E is even more tentative. The basis of this assignment lies in the similarity of the observed decay from this level to that observed in the decay of  $W^{182}$ . In the case of  $W^{182}$ , evidence is a little more certain that the corresponding level has a  $1-$  assignment.

Referring back to Plate X, all of the transition energies indicated by pointed vertical lines were observed. Many more gamma-rays were found, but as yet have not been fitted into the proposed decay scheme. It is felt that some fine structure must be superimposed upon the scheme of Plate X to accommodate the large number of weak transitions still not accounted for.

Listed in Table 1 are the observed gamma-ray energies which are felt to be reasonably well confirmed. For almost all these gamma-rays, both conversion lines and photoelectron lines were observed. In a few cases, the conversion lines were obscured by lines arising from other gamma-rays. In these cases, identification rested solely upon photoelectron lines. For energies above 180 Kev, lead radiators were employed in the photoelectron analysis. For energies below 180 Kev, both tin and molybdenum radiators were used.

As a final comment, it should be mentioned that the proposed decay scheme is not unique. Several other possible arrangements of energy levels can account for most of the observed transitions. However, the one given here appears to be most consistent, with respect to accommodating the greatest number of transitions, matching the intensity requirements of the transitions, accommodating the observed beta spectra, and finally agreeing with the Bohr-Mottelson formulation for the low lying levels.

Table 1. Energies of gamma-rays observed in Dy<sup>160</sup> decay.<sup>#</sup>

Energies in Kev.			
40.5	197*	569*	977*
43.0	214*	615*	1025*
48.6	242*	634	1034*
53.5	258	659	1110*
70.5	276*	679*	1156
77.0	285*	691	1172*
86.2*	297*	723	1186
92.6*	307	761*	1196
101.4	362	828*	1250*
115.5	391*	842	1266*
119	412*	856*	1238
136	425	862	1390
145.7	434	876*	1473
148 *	442	893	1486
155.5	460*	945	1523
179 *	508	962*	

<sup>#</sup>Most of these gamma-ray energies are thought to have a maximum error of 0.2 percent.

\*Included in proposed decay scheme.

## ACKNOWLEDGMENTS

The author wishes to express his sincere appreciation and gratitude to Dr. C. M. Fowler, for his excellent advice and helpful suggestions throughout this investigation, and especially during the preparation of this thesis. Mr. H. W. Kruse and Mr. R. J. Klotz are to be thanked for their cooperation in this investigation. Financial aid provided by the Atomic Energy Commission has been greatly appreciated.



## LITERATURE CITED

- (1) Bohr, A. and B. R. Mottelson.  
Rotational States in Even-Even Nuclei. Phys. Rev. 90: 717, 1953.
- (2) Burson, S. B., K. W. Elair and D. Saxon,  
Beta-Spectrum and Decay Scheme of  $Tb^{160}$ . Phys. Rev. 77: 403, 1950.
- (3) Cork, J. M., R. G. Shreffler, and C. M. Fowler.  
Neutron Induced Radioactivity in Certain Rare-Earth Elements. Phys.  
Rev. 74: 240, 1948.
- (4) Cork, J. M., C. E. Branyan, W. C. Rutledge, A. E. Stoddard, and J.M. LeBlanc.  
Gamma Rays from Terbium 160. Phys. Rev. 78: 304, 1950.
- (5) Davisson, C. M. and R. D. Evans.  
Gamma-Ray Absorption Coefficients. Revs. Modern Phys. 24: 79, 1952.
- (6) Klots, R. J., V. Keshishian, H. W. Kruse and C. M. Fowler.  
A Note on the Variable Radius Beta Ray Spectrometer. Rev. Sci. Inst.  
In Press. 1954.
- (7) Kruse, H. W.  
Analysis and Application of Source Tilting in a Magnetic Focusing  
Beta-Ray Spectrometer. M.S.Thesis, Kansas State College. 1952.
- (8) Muller, D. E., H. C. Hoyt, D. J. Klein and J. W. M. DuMond.  
Precision Measurements of Nuclear Beta-Ray Wavelengths of  $Ir^{192}$ ,  $Ta^{182}$ ,  
 $RaTh$ ,  $Rn$ ,  $W^{187}$ ,  $Cs^{137}$ ,  $Au^{198}$ , and Annihilation Radiation. Phys. Rev.  
88: 775, 1952.

INVESTIGATION OF THE RADIOACTIVITY  
OF TERBIUM 160

by

VAHE KESHISHIAN

B.S., Kansas State College  
of Agriculture and Applied Science, 1952

---

AN ABSTRACT OF A THESIS

submitted in partial fulfillment of the

requirements for the degree

MASTER OF SCIENCE

Department of Physics

KANSAS STATE COLLEGE  
OF AGRICULTURE AND APPLIED SCIENCE

1954

A study of the radioactivity of  $Tb^{160}$  has been made utilizing fixed field  $180^\circ$  beta-ray spectrographs, and a variable radius beta-ray spectrometer. Two unreported intense gamma-rays of 1173 and 1266 Kev were observed. Many additional weak gamma-rays were also observed. Four beta-spectra were found with energies: 851, 557, 461 and 280 Kev. Their relative abundances were 30, 32, 19 and 19 percent respectively.

The now energy level diagram proposed, accounted very well for most of the numerous transition energies observed, both with regard to energy and intensity. The beta spectra observed also substantiated the proposed scheme. In addition, the low lying levels agreed with the Bohr-Mottelson formulation.

Some investigations to determine the most effective photoelectric radiators were undertaken. It was concluded that lead was best suited for gamma-ray energies above 100 Kev, while tin and molybdenum were satisfactory for lower energies down to 30 Kev gamma-rays.